Response to Reviewers #1 and #2

We like to thank the reviewers for providing helpful comments to improve the manuscript.

We made substantial changes according to your suggestions. All changes are highlighted in the diff-mansucript below. Added text is wavy-underlined and blue, discarded text is struck out and red. There are also minor changes in some figures that are not highlighted in the diff-mansucript below. Additionally, we slightly changed the algorithms and improved the performance. Therefore, some numbers changed in the manuscript. Furthermore, we replaced the stratiform case.

The reviewer comments are listed below in black. The authors response is written in blue.

Anonymous Referee #1

General comments:

This study proposes two algorithms (PDF and ANN) for convective and stratiform precipitation separation based on the MRR measurements. The manuscript has a clear structure and smooth expression, but have some issues (e.g., weak literature survey, validation of results, the application value etc) and requires a major revision before its acceptance.

Detailed comments are provided below.

P1: In Introduction section, the authors should provide background on convective and stratiform rain in meteorological applications (e.g. Houze 2014). What are the existing methods for convective and stratiform rain separation? How the proposed algorithms on convective and stratiform rain separation has the advantage over the existing different methods? Literature survey for the artificial neural network (ANN) for rain type classification is required. The novelty of the work is not enough highlighted.

Houze, R. A., Jr. (2014) Cloud Dynamics. Academic Press.

We expanded the literature review in the introduction.

P3: Description of MRR is insufficient. Please elaborate especially the signal processing part. The Ku-band signal attenuate/extinct in convective rain. How the authors make sure about this phenomena. What signal-to-noise ratio has been considered for processing the MRR dataset

SNR is not used. In case of strong convective rain with huge drops the measured reflectivity is high and may be attenuated by the drops. Nevertheless the reflectivity is expected to be too high to erroneously classify the rain to be stratiform. We added this explanation in sub-section 3.2.

P4: Ln 4: In stratiform case, the Zmax will be at the melting layer (bright band). Do the authors consider this factor in their analysis?

Therefore we use three variables instead of only one. In case of cold stratiform rain with high Zmax values in the melting layer the other two variables which are not affected by the bright band will force the retrievals (PDF and ANN) to classify stratiform rain. We added this explanation.

Up to what height, the analysis is performed?

The analysis is performed up to 3 km. We added this explanation.

P4: Ln 8: On what basis 15 min time interval is taken?

It is a reasonable time span for convective rain. If the rain shower is shorter than 30 min (plus minus 15 min) the shorter time span is used to derive the variability. We added this explanation.

P4: Ln11: On what basis the scores/weight are defined in Figure 1? Is threshold values of weight are region-specific? Which dataset is used to calculate the soaring index (S), convection index (Ko), total totals (TT)? What is the temporal and spatial resolution of those data?

We found that the variability of the Doppler velocity is the most reasonable measure to distinct between stratiform and convective rain. Therefore this measure was assigned the highest weight. The model data from COSMO (temperature and humidity profile) differ too much if the nearest model grid point is a grid point with precipitation or without precipitation. Therefore, the model derived measures as TT, KO, and So got smaller weights, because the measured variables are more trustworthy than the modeled ones. We added missing model information.

P4: Ln 21: On what basis the convection score partition (stratiform less than 3, inconclusive 3-6 and convective >6) is taken? Does the author consider the rain rate criteria also?

These values are chosen to have a big transition (inconclusive) zone between stratiform and convective. This is a very strict separation. In this way the probability of false classification is very low and the data set is prepared for training the algorithms. The huge amount of inconclusive cases is not part of interest here. We added missing information. Additionally, the upper threshold was set to 5.5 to increase the amount of profiles that are assigned as convective.

P5: Figure 2: The inconclusive data points are more than the convective and stratiform samples. Please comment on it? Whether the inconclusive samples are the transition from convective to stratiform event.

Yes inconclusive cases are the transition between both classes. See comment above.

P5: Ln 3: … visual classification of each single profile. How the authors have visually classify the profile into convective and stratiform? What parameter and criteria are used for the visual classification? Please provide a skill score table for better representation of your results.

We had a detailed view on randomly selected cases, if the classification using the convection score worked well. We checked the synoptic situation and had a look at the mentioned variables. We added missing information according to your suggestions.

P10: Figure 6: Out of two proposed algorithms (PDF and ANN), which method is superior? Authors also need to discuss the source of errors for each method. In the manuscript, the evaluation of the precipitation classification algorithms is not shown.

We restructured the algorithm comparison part with a new figure (Fig. 7, now Fig. 8). Thereby we improved the discussion of the results including misclassifications according to you suggestions.

Please provide some discussion on the proposed algorithm and related future research to put the results into a broader context.

We improved the discussion and outlook part.

Minor:

P2: Ln25: … following section. Change to sub-section.

Done as suggested.

P5: Ln 10: Zmax up to 50 dBZ. Don't you think there will be attenuation at such high reflectivity value?

We use the radar reflectivity factor Z calculated from the drop size distribution (and Doppler spectra) and not the measured reflectivity Z_e. It is not affected by attenuation. Anyways, Zmax of up to 40 dBZ occured only rarely and do not influence the results significantly.

P6: It will be good to show the rainfall distribution like figure 3d.

We included Fig. 3 in Sec. 3.2 which shows the frequency distribution of stratiform and convective precipitation at 300 m height according to your suggestions.

P7: What bin size the authors have considered for Eq. (4) and (5).

We added the missing information to the text.

P11: Figure 7: PDF is overestimating the convective and stratiform precipitation than ANN. Which result is more accurate. For the inconclusive sample, both the methods have the same occurrence frequency. Why the number of data sample (NPDF and NANN) for analysis are different.

We restructured the comparison part and replaced Fig. 7 (now Fig. 8). We improved the discussion according to the reviewers suggestions.

Anonymous Referee #2

General comments:

The study discusses the two algorithms PDF and ANN for classifying convective and stratiform precipitation profiles based on MRR data. The authors utilizes the maximum reflectivity, mean Doppler velocity and maximum deviation in velocity within +/- 15 min. But there have been a numerous studies on this topic using various ANN based algorithms (e.g., Ghada et al., 2019, doi:10.3390/atmos10050251, Jergensen et al., 2020, DOI: 10.1175/WAF-D-19-0170.1).

We expanded the literature review.

The paper is topic of interest. The authors presented only two algorithms. It could have been good to show the results from various ANN based models to discriminate the convective and stratiform profiles and compare them.

This is not the scope of the paper. We aim for an algorithms based only on MRR observations to enable a wide spread and straightforward usage for ground-based remote-sensing sites.

Further, authors should include the validation metrics such as RMSE, MAPE, etc in tabular form for both the models.

The pdf method doesn't produce validation metrics. The results are visualized in Fig. 7 and discussed in the corresponding section. Nevertheless, we improved the discussion part by adding more information on the performance of both methods compared to the convection score. See more detailed comments below.

Perhaps, use of convolution neural networks (CNNs), Long-short Term Memory (LSTM) and recurrence neural networks (RNNs) will provide better forecast for time series data.

Yes, this could be. However, our methods provide satisfactory results.

However, I concern about following comments. I recommend that this manuscript requires major revision before its acceptance.

Detailed comments are provided below:

P2: Why authors are used two year data for training? Is this data covers the all dynamic ranges observed convection/stratiform? Any ANN based model, the training data should have the all range of values.

Actually, we use just one year 2013 for training. In principle you are right, more training data would improve the ANN accuracy. In future, we will apply the retrievals at our remote sensing site at University of Leipzig. Currently, we are observing 24/7 with our MRR. So the amount of data is increasing and we will have the opportunity to improve the algorithms with new data. We added that part about our future activities in the outlook of the paper.

P3: Are three indices such soaring index (S), convection index (Ko), total totals (TT) derived using COSMO model data? If so, is COMSO derived indices are validated with indices calculated form radiosonde observations?

Yes, based on COSMO-EU, but it is not validated with radiosondes since there are no radiosonde launches at JOYCE on regular basis. We added some information about the COSMO-EU model such as resolution.

P3:L5: Why the authors are used 15 minutes interval, where MRR gives 1 minute data?

We didn't use a 15 min time interval. We use 1 minute but calculate the temporal standard deviation of the maximum Doppler velocity (per profile) based on plus minus 15 minutes time span. It is a reasonable time span for convective rain.

P4.L6-7: … convective precipitation contains larger rain drops … Is it true always?
Include reference.

We added Niu et al. (2020) as reference and rephrased the sentence.

P4.L8-9: … +/-15 min is a reasonable time span for classification of rain events … But, there are the occasions, where the life time of convection will be less than 15 minutes. Authors should modify the sentence. Include reference.

In case of shorter rain showers the standard deviation is calculated on the shorter time span. In any case the standard deviation of the Doppler velocity is higher than during homogeneous stratiform rain. We added an explanation to the text.

P5.L9: … PDF and ANN method are based on training, the data has to be free of extreme or unphysical values … Do authors mean that the data cleansing? I understood that the data filter was performed in MRR data. If so, rewrite the sentence. However, what are the extreme values? Because, in general, if the trained data consists of all dynamics range, then the model will be able to predicted with better accuracy.

We rephrased the sentence to clarify misunderstandings.

P5:L24: What are the modification are done in Liu et al. (2004) and Liu et al. (2009) algorithms.

We rephrased the paragraph and added missing information.

P6:L23-24: … the confidence of a discrimination algorithm can be improved by using three measurement variables instead of only one or two … Are the proposed number of variables are sufficient? Is the model predicting better accuracy, if you consider more than three input variables? Is the prediction depends on number of depended variables? Why authors are not consider rain rate for training MLP model?

Yes, the model accuracy depends on the number of dependent variables. We do not consider rain rate, since rain rate and reflectivity are calculated using rain drop number concentration. There will be no additional independent information. We added these information to the text.

P8:L16: Is the MLP model is multivariate multi-step? I also suggest including a table with hyperparameters of MLP used in this study, rather than mentioned in the text.

Since the MLP is a categorization model the most meaningful quantity for the estimation of uncertainty are categorical cross entropy to calculate the loss, and the categorical accuracy. RMSE or MAPE are not suitable for the description of the categorical model since it gives probabilities to be stratiform, inconclusive or convective.

The authors did not give an overview about the hyper parameters in a table since Fig. 5 gives most information about the ANN setup. All other information such as accuracy are given in the brief ANN section.

P9: For readers, change line colour to red in figure 6 (m) & (n).

We improved the entire figure according to your instructions.

P9: I would rather suggest to include about “how often convective/ stratiform/inconclusive profiles occur at JOYCE supersite?

The numbers are given in Fig.2. We added that information for the test data set 2014 in the new figure 7.

P11: The relative occurrences of inconclusive profiles are equally weighting with convective/ stratiform in this study? Are they meant for transition profiles?

We completely changed and improved the evaluation of the algorithm performances. It is more clear now.

Evaluation of micro rain radar-based precipitation classification algorithms to discriminate between stratiform and convective precipitation

Andreas Foth[1], Janek Zimmer[2], Felix Lauermann[1,3], and Heike Kalesse[1]

[1]Leipzig Institute for Meteorology, University of Leipzig, Leipzig, Germany
[2]Meteologix AG, Sattel, Switzerland
[3]now at: Deutscher Wetterdienst, Meteorologisches Observatorium Lindenberg/Richard–Aßmann–Observatorium, Tauche, Germany

Correspondence: Andreas Foth (andreas.foth@uni-leipzig.de)

Abstract. In this paper, we present two micro rain radar-based approaches to discriminate between stratiform and convective precipitation. One is based on probability density functions (PDFs) in combination with a confidence function and the other one is an artificial neural network (ANN) classification. Both methods use the maximum radar reflectivity per profile, the maximum of the observed mean Doppler velocity per profile and the maximum of the temporal standard deviation ($\pm 15\,\mathrm{min}$) of the observed mean Doppler velocity per profile from a micro rain radar (MRR). Training and testing of the algorithms were performed using a two year data set from the Jülich Observatory for Cloud Evolution (JOYCE). Both methods agree well giving similar results. However, the results of the ~~artificial neural network are more reasonable~~ ANN are more decisive since it is also able to distinguish into an inconclusive class, in turn making the stratiform and convective classes more reliable.

1 Introduction

Evaporation of precipitation below cloud base is a crucial process in the water- and energy cycle. Precipitation can be of two clearly distinguishable types – stratiform and convective. Both types originate from different clouds (Houze Jr, 2014). Stratiform precipitation mainly falls from nimbostratus whereas convective precipitation originates from active cumulus and cumulonimbus clouds. These cloud types may occur separately or entangled in the same cloud complex.

The parameterization of ~~this~~ the precipitation evaporation process is highly empirical in current general circulation models (Rotstayn, 1997). Evaporation of precipitation generates cold pools that lead to convective organisation (Schlemmer and Hohenegger, 2014) and Tropical storms (Pattnaik and Krishnamurti, 2007); it is highly relevant for boundary-layer humidity (Worden et al., 2007) and subsequently for the Tropical general circulation (Bacmeister et al., 2006). However, also in the midlatitudes, precipitation evaporation is an important factor in the water cycle (Morrison et al., 2012) and the simulated water cycle processes are highly sensitive to the empirical parameters and assumptions.

In order to improve the parameterization of evaporation from convective rain a big data set of convective rain cases is needed to generate robust statistics. Since it is a large effort to manually discriminate between stratiform and convective cases, automated algorithms were developed.

In previous approaches~~Caracciolo et al. (2006) separated~~ , stratiform and convective rain are separated based on the rain drop size distribution measured by a disdrometer (Caracciolo et al., 2006; Thompson et al., 2015; Ghada et al., 2019). Precipitation was also classified using radar images and radar wind profiler data (Rosenfeld et al., 1995; Williams et al., 1995; Tokay and Short, 1996; Tokay et al., 1999; Yang et al., 2013). Deng et al. (2014) classified convective precipitation based on thresholds of the radar reflectivity and the gradient of accumulative radar reflectivity retrieved from a vertically pointing cloud radar. Geerts and Dawei (2004) used a decision tree to separate different precipitation types by means of cloud radar variables. ~~Yang et al. (2019) developed a discrimination algorithm~~ Additionally, discrimination algorithms using an ANN ~~.~~ were developed (Yang et al., 2019; Ghada et al., 2019) . The ANN approach of Yang et al. (2019) is based on ground-based Doppler Radar observations. Lazri and Ameur (2018) combined a support vector machine, ANN and random forest to improve the stratiform convective classification using spectral features of SEVIRI data. Jergensen et al. (2020) classify thunderstorms into three categories: supercell, part of a quasi-linear convective system, or disorganized using radar data in a machine learning approach.

In summary, several approaches such as ANN, fuzzy logics, or decision trees based on different instruments such as disdrometer, cloud radar, precipitation radar, or radar wind profiler were developed in the past. In this paper, two methods are developed which classify rain as stratiform or convective event based only on MRR observations to enable a wide spread and straightforward usage for ground-based remote-sensing sites.

2 Instrumentation

2.1 Supersite JOYCE

In recent years, the Jülich Observatory for Cloud Evolution (JOYCE[1]) was equipped with a combination of synergistic ground-based instruments (Löhnert et al., 2015). JOYCE is situated at $50°54'31''$N and $6°24'49''$E with an altitude of 111 m MSL. In 2017 JOYCE was transformed into a Core Facility (JOYCE – CF) funded by the DFG (Deutsche Forschungsgemeinschaft) with the aim of high quality radar and passive microwave observations of the atmosphere. The supersite operates a variety of ground-based active and passive remote sensing instruments for cloud and precipitation observations, for example: X, Ka, and W-Band radars, ceilometers, a Doppler wind lidar, an atmospheric emitted radiance interferometer (AERI), a Sun photometer,

[1]JOYCE webpage: http://cpex-lab.de/cpex-lab/EN/Home/JOYCE-CF/JOYCE-CF_node.html, last accessed: ~~2020-07-16~~2020-12-01

disdrometers, several radiation measurement systems, as well as an MRR. The latter is the main instrument in this study and is explained in detail in the following ~~section~~sub-section. The data used in this study was gathered in 2013 and 2014. The data from 2013 covers the entire year and was used to train the algorithms (training data set). The data from 2014 covers almost the entire year apart from February. It is ~~completely independent~~ a completely independent data set and is used as test data set for the algorithms. In 2013 and 2014, 471 and 683 hours of rain were observed, respectively.

2.2 Micro rain radar

The micro rain radar (MRR) which is built by the Metek (Meteorologische Messtechnik GmbH) company, is a compact FM-CW (frequency modulated-continuous wave) Doppler radar operating at 24 GHz (Peters et al., 2002). The MRR at JOYCE (in 2013 and 2014) ~~was operated with 31 range gatesfrom 100 to 3100~~is an MRR-2 system operating with 32 range gates. The lowermost range gates (number 0, 1 and 2) up to 200 m ~~resulting in a vertical resolution of 100~~are affected by near-field effects and the last range gate of 3100 m ~~. The~~ is too noisy. These range gates are usually omitted according to Maahn and Kollias (2012). Hence, 28 range gates from 300 to 3000 m remain for the analyses in this study. The vertical and temporal resolution amounted to 100 m and 1 min, respectively. The MRR data was processed according to Peters et al. (2005). The instrument was zenith pointing and measured the radar Doppler spectrum from which the ~~attenuated equivalent reflectivity Z and the~~ mean Doppler velocity (v_{D}) were derived. The radar reflectivity factor (Z) is derived via integrating over the drop size distribution according to Peters et al. (2005).

3 Stratiform convective discrimination

3.1 Convection indices

Several weather indices can be used to describe the stability of the atmosphere (Kunz, 2007). Three indices ~~are~~ that are based on thermodynamic profiles are described in the following. All give a hint on the probability of convection based on COSMO (Consortium for Small-scale Modeling) EU model data. ~~The~~ COSMO-EU has a horizontal resolution of 7 km and a vertical resolution between around 60 m and 370 m below 3 km. The temporal resolution amounts to 1 h. The weather index total totals is a combination of the vertical totals (VT) and cross totals (CT). The VT is the temperature (ϑ in ° Celsius) difference between 850 hPa and 500 hPa while the CT is 850 hPa dewpoint (τ) minus the 500 hPa temperature:

$$\begin{aligned} TT &= VT + CT \\ &= (\vartheta_{850} - \vartheta_{500}) + (\tau_{850} - \vartheta_{500}). \end{aligned} \tag{1}$$

The higher the TT, the more probable is convection.

The second index, named KO index (Andersson et al., 1989), describes the potential instability between lower and higher

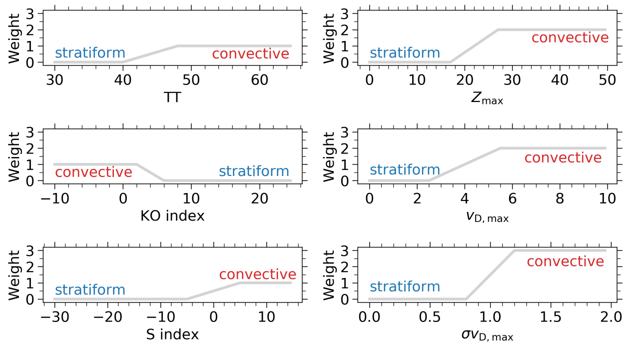

Figure 1. Weight of the meteorological and radar-based convection criteria: ~~soaring index~~ total totals ($\cancel{S}TT$), convection index ($\cancel{Ko}KO$), ~~total totals~~ soaring index ($\cancel{TT}S$), maximum of the reflectivity (Z_{max}) per profile, maximum of the Doppler velocity ($v_{\mathrm{D,max}}$) per profile and the maximum (per profile) of the temporal standard deviation of the Doppler velocity ($\sigma v_{\mathrm{D,max}}$) within a ± 15 min interval.

levels of the atmosphere (at 1000 hPa, 850 hPa, 700 hPa, and 500 hPa). It is thus based on the pseudo-potential temperatures θ_e:

$$KO \quad = \quad 0.5\,(\theta_{e,700} + \theta_{e,500} - \theta_{e,1000} - \theta_{e,850}). \tag{2}$$

The lower the KO index the higher the ~~probability~~ potential of convection.

The soaring index[2] (S) is intended to be a tool in soaring and sporting aviation because it gives a hint on thermal lift and hence on instability. It is defined as:

$$S \quad = \quad \vartheta_{850} - \vartheta_{500} + \tau_{500} - (\vartheta_{700} \cancel{\pm} - \tau_{700}). \tag{3}$$

The higher the S index the higher the probability of convection.

3.2 Convection score

First, a convection score to classify three types of precipitation ~~,~~ labelled as stratiform, convective and inconclusive, is defined by applying a threshold range to six different variables. Three variables are based on thermodynamic profiles ($\cancel{S}TT$, KO, $\cancel{TT}S$) and three are based on the MRR observations. Specifically, the used MRR variables are: the maximum of reflectivity (Z_{max}) per profile, maximum of the mean Doppler velocity ($v_{\mathrm{D,max}}$) per profile and the maximum (per profile) of the temporal standard deviation (~~±~~ ± 15 ~~15~~ min) of the mean Doppler velocity ($\sigma v_{\mathrm{D,max}}$). The profile maxima are calculated between ground and 3 km. It is expected that ~~convective precipitation contains~~ larger rain drops ~~resulting in~~ are usually caused by convective precipitation (Niu et al., 2010) which leads to higher Z and v_{D} values, respectively. Furthermore, stratiform precipitation is expected to be less variable over time whereas convective precipitation results in a larger standard deviation of v_{D} over time. It ~~was shown~~ is assumed that $\pm$ 15 min is a reasonable time span for classification of rain events. If the rain event is shorter

[2] http://www2.wetter3.de/soaring_index.html, last accessed: ~~2020-07-16~~ 2020-12-01

than 30 min ($\pm$15 min) the variability is determined over this shorter period. The maxima of the height dependent Z, v_D and σv_D are used to assign the vertical properties to profile properties. In case of cold stratiform rain there might be a clearly defined melting layer. The so-called radar 'bright band' is indicated by erroneously high reflectivity values Z in the layer of melting ice particles which force the detection to be convective. Therefore, two other variables (v_D and σv_D) are chosen which are not affected by the melting layer and both will counteract the false classification and force the retrieval to classify stratiform.

~~The variables have different weightings~~ Different weightings are assigned to the six variables as visualized in Fig. 1. Whenever a variable exceeds a convection threshold range (or falls below in case of KO index), the weight to be convective increases. The weightings of all variables are summed up resulting in the convection score. The application of a smooth linear threshold range of weights between stratiform and convective is more realistic ~~than using strict binary thresholds which finally~~ and leads to a more homogeneous distribution of the convection score compared to using strict binary thresholds. By using six variables the classification is more robust against false classifications than those based on one single variable. The MRR-based variables have a stronger weighting than the model-based variables due to their smaller uncertainties. ~~The weight of~~ $\sigma v_\mathrm{D,max}$ ~~has~~ is assigned to have the highest weight because the variability of the rain intensity is assumed to be the best criterion for the stratiform-convective discrimination.

Figure 2 illustrates the distribution of the convection score. Whenever a convection score is less than 3 the profile is assigned to be stratiform. Values between 3 and ~~6~~ 5.5 are stated as inconclusive. Values larger than or equal to ~~6~~ 5.5 are assigned as convective. These strict thresholds enable a very certain classification with a low amount of false classifications. The inconclusive zone between stratiform and convective indicates a transition between both. The thresholds of 3 and 5.5 were chosen to confidently separate two classes which are mainly free of false classified rain events resulting in a confident data set for training the algorithms. This approach replaces a manual ~~classification~~ inspection by visual classification of each single profile. However, several rain events were reviewed by eye to verify a correct classification. That means randomly selected cases were checked if the convection score worked as intended and the synoptic situation was reviewed.

At this step, each profile is either classified as stratiform, inconclusive, or convective using the convection score and this assignment is stated as true state to train the algorithms explained below. Since the motivation of this work is to classify the precipitation type and its confidence ~~only~~ purely based on the MRR observations the following methods based on PDFs or ANN are ~~deployed~~developed. Since the PDF and ANN method are based on training, the MRR data has to be free of extreme or unphysical values. Therefore the ~~data~~ MRR data (input) is filtered. Only measurements with Z_max between -10 and 50 dBZ, $v_\mathrm{D,max}$ between 0 and 10 $\mathrm{m\,s^{-1}}$ and $\sigma v_\mathrm{D,max}$ between 0 and 2.5 $\mathrm{m\,s^{-1}}$ are taken into account.

Here, the question might arise why inconclusive profiles should be learned by algorithms. In fact, rain events can be ambiguous and cannot be classified into stratiform or convective, especially stratiform rain moving towards mountainous area which causes convection. On the other hand, vertical air motion and turbulence influence $v_\mathrm{D,max}$ and might shift stratiform

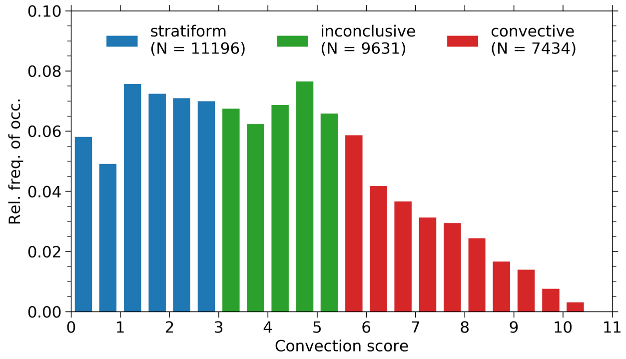

Figure 2. Relative frequency of occurrence of the ~~convective~~ convection score.

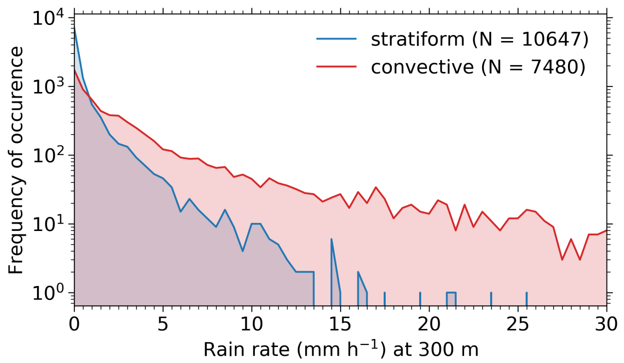

Figure 3. Frequency of occurrence of rain rate at 300 m height for stratiform (blue) and convective (red) rain cases.

profiles towards higher convection scores and convective profiles to lower scores. A class with inconclusive profiles accounts for the mentioned features and avoids misclassifications into the stratiform and convective classes, respectively.

The frequency distribution of rain rate at 300 m height is shown in Fig. 3. The precipitation cases are separated by the convection score. The stratiform precipitation mostly causes low rain rates below 1 mm h^{-1} whereas high rain rates above 15 mm h^{-1} are very rare. In contrast, high rain rates above 15 mm h^{-1} are caused by convective precipitation. It has to be considered that the absolute number of occurence differ from Fig. 2 because precipitation disappears due to evaporation on the way through the atmosphere and is not reaching 300 m which is the lowest available MRR height.

3.3 Rain classification method based on PDF

This algorithm was developed based on the classification ~~algorithms by Liu et al. (2004) and Liu et al. (2009) which were~~ algorithm by Liu et al. (2004) which was originally developed for the Cloud-Aerosol Lidar and Infrared Pathfinder Satellite

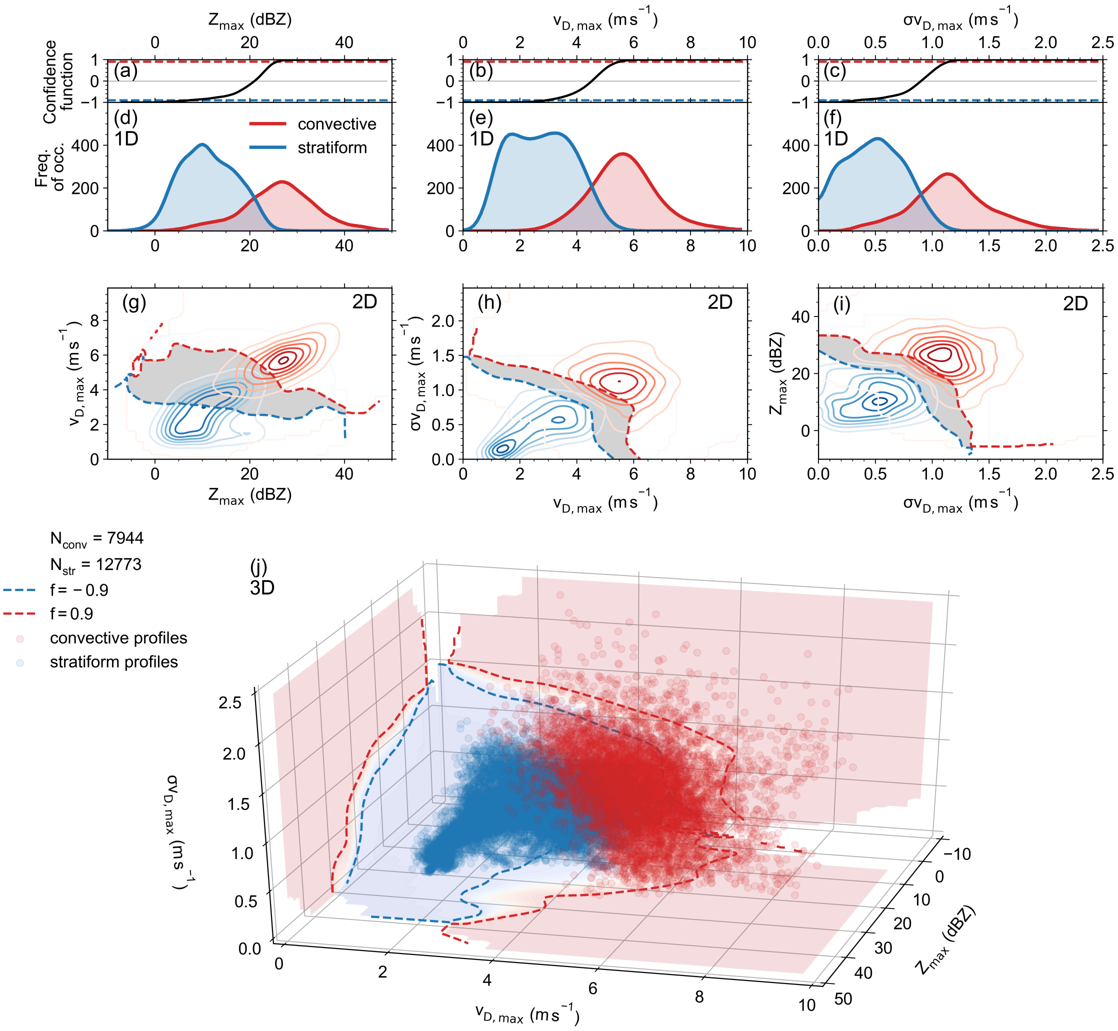

Figure 4. Overview about the one-dimensional (1D~~,~~:d,e,f), two-dimensional (2D~~,~~:g,h,i), and three-dimensional (3D~~,~~:j) probability density functions for the maximum radar reflectivity $Z_{\max}$ per profile (d), the maximum of the observed Doppler velocity $v_{\mathrm{D,max}}$ per profile (e), the maximum of the temporal standard deviation of the observed Doppler velocity $\sigma v_{\mathrm{D,max}}$ per profile (f), and each 2D combination of these three variables (g-i). (j) shows the 3D scatterplot of the three variables with the contour of the corresponding confidence values in each plane. (a-c) show the ~~the~~ confidence function of the corresponding 1D distributions. The dashed lines represent the thresholds of a confident classification with values beyond -0.9 and 0.9, whereas values in between are indicated by a grey area (g-i). Stratiform or convective profiles are indicated by blue or red colours and by low or high values of the confidence functions, respectively.

Observations (CALIPSO) aerosol cloud discrimination (Winker et al., 2009). It shows that the confidence of a discrimination algorithm can be improved by using three measurement variables instead of only one or two. Later on, Liu et al. (2009) improved the algorithm by using five instead of three variables. Here, this separation approach is modified for MRR variables to classify precipitation into stratiform or convective.

The confidence function is defined as:

$$f(X) = \frac{n_c(\boldsymbol{X}) - n_s(\boldsymbol{X})}{n_c(\boldsymbol{X}) + n_s(\boldsymbol{X})} \tag{4}$$

$$= \frac{P_c(\boldsymbol{X}) - P_s(\boldsymbol{X})/N_s/N_c}{P_c(\boldsymbol{X}) + P_s(\boldsymbol{X})/N_s/N_c} \tag{5}$$

with n_i being the number of occurrences of class i (stratiform s or convective c) having attribute X and N_i the total number of events for the ith class. P is the PDF of $\boldsymbol{X}$ which can be multidimensional $\boldsymbol{X} = [X_1, \ldots, X_m]$. The used bin size of the distributions of Z, $v_{\mathrm{D,max}}$, and $\sigma v_{\mathrm{D,max}}$ amounts to 0.5 dB, 0.125 $\mathrm{m\,s^{-1}}$, and 0.025 $\mathrm{m\,s^{-1}}$, respectively. The value of f is bounded ~~on~~ by [-1,1]. The lower the value, the more probable the MRR-observed rain profile is ~~to be stratiform~~ of stratiform nature. Values of exactly -1 are treated as certainly stratiform and values of $+1$ correspond to certainly convective profiles. Values around 0 indicate uncertain classifications. On the basis of the return value of f a classification and a measure of the confidence of this classification can be derived. The sign of f determines the class assignment and the absolute magnitude of f assigns the confidence to the classification. In the following the PDFs are smoothed using a Gaussian filter with a standard deviation of 3 bins in each dimension to account for gaps in the PDF due to missing variable ~~combination~~ combinations in the training data. Applying such a Gaussian filter makes the PDF method more robust.

Figure 4 (d), (e) and (f) ~~shows~~ show the one-dimensional distribution of the three MRR variables (Z_{max}, $v_{\mathrm{D,max}}$ and $\sigma v_{\mathrm{D,max}}$) and their corresponding confidence functions f (a,b,c). Here, the stratiform and convective precipitation profiles are distinguished by the convection score explained above. However, Z_{max} at values between ~~5 and 25~~5 and 25 dB shows a region of overlap between both classes resulting in low magnitude of f ~~with values~~ ranging between -0.8 and ~~0.8~~0.8. Z_{max} below ~~5~~5 ~~dB or above 25~~dBZ or above 25 ~~dB~~ dBZ can be reliably classified as stratiform or convective, respectively (Fig. 4 d). The distribution of $v_{\mathrm{D,max}}$ (Fig. 4 e) as well as $\sigma v_{\mathrm{D,max}}$ (Fig. 4 f) ~~shows a significant overlap region between 2.5 and 5.5~~show significant overlap regions between stratiform and convective profiles between 2.5 and 5.5 $\mathrm{m\,s^{-1}}$ and between ~~0.2 and 0.8~~0.4 and 1.1 $\mathrm{m\,s^{-1}}$, respectively. This results in absolute magnitudes of f below ~~0.8. Since~~ 0.8 for both v_{D}-related variables. The overlap area of stratiform and convective profiles is smallest for $\sigma v_{\mathrm{D,max}}$ but since vertical air motion and turbulence influence $v_{\mathrm{D,max}}$, it ~~thus~~ can not serve as stand-alone value. In conclusion, a classification algorithm based on only one of the mentioned MRR variables is not able to unambiguously distinguish between stratiform and convective precipitation indicated ~~by the~~ due to existing overlap regions.

The ambiguity can be reduced by adding a second dimension to the PDF. Figure 4 (g), (h) and (i) illustrate the distribution of each two-dimensional (2D) combination of the three MRR-based variables. The dashed lines indicate the f values of -0.9 and 0.9. The values in between represent the overlap where no unambiguous assignment can be made (grey area). The peaks of the two classes are clearly separated for all three variable combinations (g,h,i). Nevertheless, there are still observations leading to an ambiguous assignment. In principle, these ambiguous assigned profiles with f values between -0.9 and 0.9 could be stated

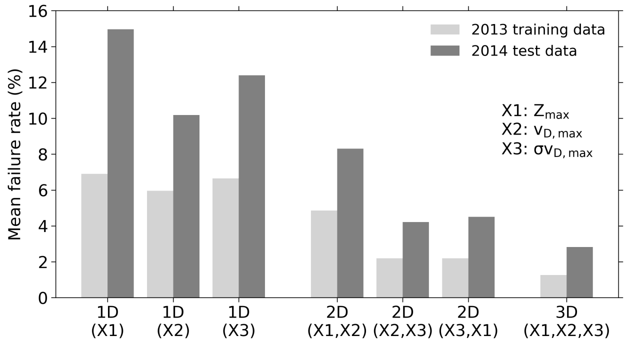

Figure 5. ~~The~~ Comparison of the mean stratiform convective discrimination failure rates ~~contrasted between~~ for two data sets, the training data set from 2013 (light grey) and the test data set from 2014 (dark grey). The shown failure rate is separated for PDFs with increasing dimension: 1D is based on only one MRR variable, 2D is a two dimensional PDF based on two MRR variables and, 3D is a three dimensional PDF based on three MRR variables, as mentioned in the legend.

as inconclusive. However, the PDF algorithm is not trained to classify inconclusive cases. A quantitative estimation of how well the discrimination works is given at the end of this ~~section~~sub-section.

By using all three mentioned MRR-based variables a three-dimensional (3D) PDF can be created which is visualized in Fig. 4 (j). It is indicated that both stratiform and convective profiles are clearly separated with a very small region of overlap. The quality of the 3D PDF-based classification in contrast to 2D and 1D can be explained in terms of failure rates R_f (Liu et al., 2009):

$$R_\mathrm{f}(\boldsymbol{X}) \quad = \quad \frac{|f(\boldsymbol{X})-1|}{-2}. \tag{6}$$

As explained above the performance of the classification is limited by the amount of overlap in the PDFs. The smaller the overlap, the more clear is the separation between stratiform and convective profiles. Figure 5 presents the mean failure rate for the 1D-, 2D-, and 3D PDFs of the training data set 2013 and the independent test data set 2014. The training data was used to build the PDF for the calculation of f. For each profile from the test data, the according f value can be read out from the trained confidence function. To account for measurement uncertainties ~~and turbulence incluencing~~ or turbulence influencing all radar variables, the f underlying PDFs are smoothed using a Gaussian filter with a standard deviation of 3 bins in each dimension corresponding to a Z_max of 1.5 dB, $v_\mathrm{D,max}$ of 0.38 $\mathrm{m\,s^{-1}}$, and $\sigma v_\mathrm{D,max}$ of 0.08~~. It can be seen~~ $\mathrm{m\,s^{-1}}$. In Fig. 5 it is obvious that a reduction of the overlap by adding another attribute (MRR-based variable) results in smaller failure rates. Highest failure rates result from the 1D-PDFs. The mean failure rate for the 3D-PDF based rain classification discrimination for training and test data is less than 1 % and 3 %, respectively. This is much lower than the failure rates of 1D and 2D PDFs for stratiform-convective discrimination, which range between 2 to ~~9~~7 % for the training data set and 3 to ~~16~~15 % for the test data set.

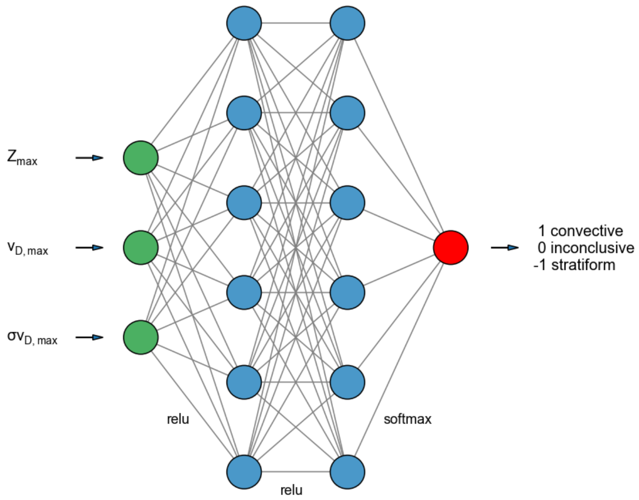

Figure 6. Diagram of the neural network with an input layer consisting of three nodes (green) according to the three MRR-based variables, two hidden layers with six nodes each (blue) and the output layer with one node (red).

It was shown that the algorithm performance could be improved by adding more variables. However, the amount of independent variables only obtained by MRR is limited. Z calculation is based on the drop number concentration. Other MRR variables such as rain rate or liquid water content are also based on drop number concentration and are hence not independent from Z and would not add any more information to the discrimination algorithm.

3.4 Method based on an artificial neural network (ANN)

A classification of rain as stratiform, convective or inconclusive can also be based on an ANN. The ANN model used here is a multi-layer perceptron approach implemented using the open source machine learning library for research and production *TensorFlow*[3]. It is trained with $Z_{\max}$, $v_{\mathrm{D,max}}$ and $\sigma v_{\mathrm{D,max}}$ from the training data set (2013). The ANN model (Fig. 6) consists of 3 input nodes ($Z_{\max}$, $v_{\mathrm{D,max}}$ and $\sigma v_{\mathrm{D,max}}$) and is further composed of two hidden layers with 6 nodes each, and one output node to learn how to classify rain events according to the true classification made by the convection score. Giving $Z_{\max}$, $v_{\mathrm{D,max}}$ and $\sigma v_{\mathrm{D,max}}$ as input to the ANN it will classify the rain event with probabilities to be stratiform (labeled as -1), inconclusive (0), and convective (1). To finally classify the rain event the class with the highest probability is stated to be the actual rain type. The model is trained for ~~300~~ 500 epochs (iteration steps) and the training data is shuffled before each epoch. The algorithm *Adam*[4] is used to optimize the model. As activation functions relu (rectified linear unit) and softmax are used for the two hidden layers and the output layer, respectively. Relu avoids negative output whereas softmax produces an output which is a range of values between 0 and 1, with the sum of the probabilities been equal to ~~1.~~ 1. As loss function the categorical cross-entropy is used to

[3]TensorFlow: An end-to-end open source machine learning platform, https://www.tensorflow.org/, last accessed: ~~2020-07-16~~2020-12-01

[4]Kingma, D.P. and Ba, J.: Adam: A Method for Stochastic Optimization, 2014. web: https://arxiv.org/abs/1412.6980, last accessed: 2020-12-01

compute the cross-entropy loss between the truth and the predictions. The cross-entropy is a measure of the difference between two probability distributions. The accuracy of the neural network can be described in terms of how often the predictions ~~equals~~ equal the truth. The ANN accuracy ~~referred to a validation data set, which is a subset of a tenth of randomly chosen 2013 data, exceeds 92~~of the independent test data set (2014) amounts to 80 %. ~~Giving Z_{max}, $v_{\mathrm{D,max}}$ and $\sigma v_{\mathrm{D,max}}$ as input to the ANN it will classify the rain event with a probability to be stratiform (labeled as -1), inconclusive (0) or convective (1).~~

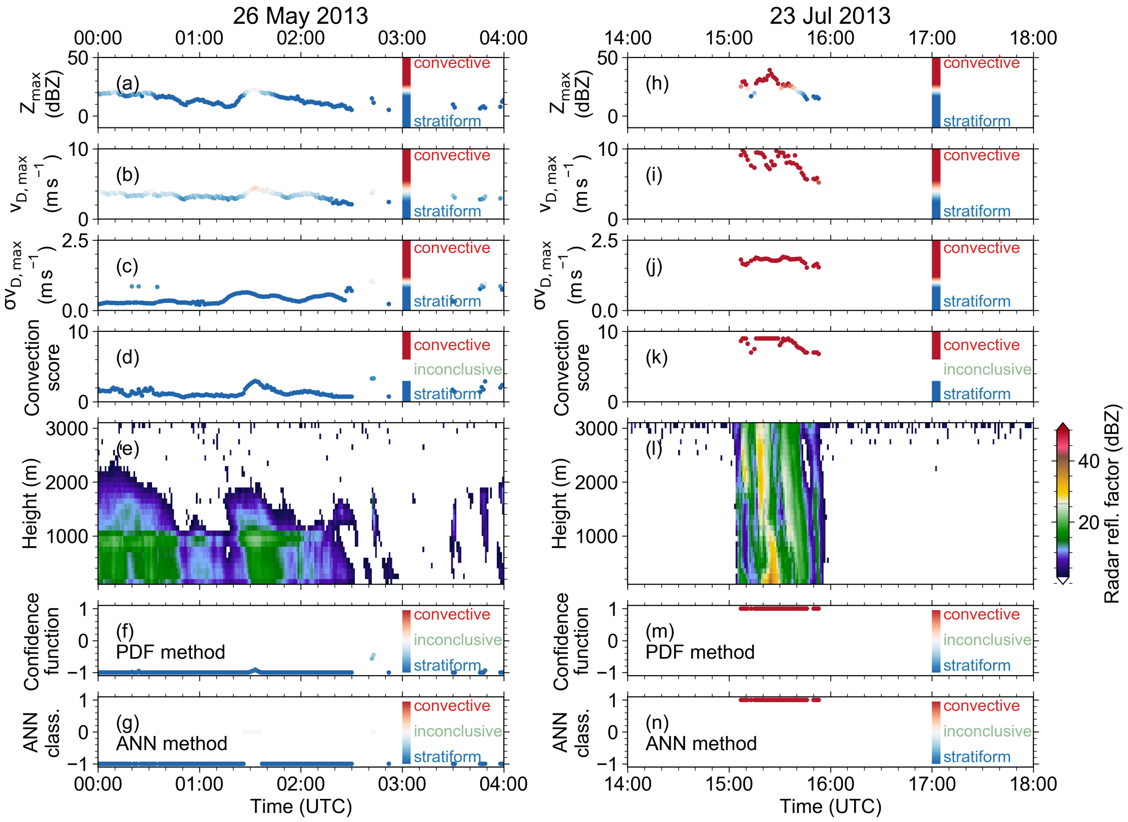

Figure 7. Discrimination indices: Z_{max} (a,h), $v_{\text{D,max}}$ (b,i), $\sigma v_{\text{D,max}}$ (c,j) and the convection score indicating the true rain type (d,k). MRR reflectivity (e,l) and the rain classification based on the PDF method given by the confidence function (f,m) and based on the ANN (g,n). The ~~color bars within~~ data points in the time series ~~illustrate~~ are coloured according to the convection criteria whether the values indicate ~~strafitform~~ stratiform or convective rain. Left panels ~~are from 11 February 2013 and~~ refer to the case study of 26 May 2013, right panels ~~are from~~ show 23 July 2013.

4 Results

After the successful development and evaluation of the classification algorithms, both the 3D-PDF-based and the ANN were applied to two case studies. The first one was a rainy ~~day on 11 Feb~~ night on 26 May 2013 (Fig. 7 a-g). Figure 7 (e) shows the time–height display of the ~~attenuated equivalent reflectivity . During the day there were four rain events at around 6:~~radar reflectivity factor. The day began with rain from 00~~, 10~~:00~~, 11:00 and 15:00~~ UTC to 02:30 UTC. The rain fell homogeneously with ~~quite constant~~ only small variations in Z_{max} (a), $v_{\text{D,max}}$ (b) and $\sigma v_{\text{D,max}}$ (c). The calculated convection score (d) was very low which means that these rain events were stated to be stratiform. ~~The PDF-based algorithm classifies each single profile as stratiform apart from two outliers at 12:30 UTC (Fig. 7 f). The ANN classifies all profiles as stratiform except for the outliers from the PDF method. Those are classified as inconclusive which is more reasonable in this context. For these wintertime~~ For this springtime rain events, the ~~ANN and PDF~~ PDF (f) and ANN (g) method produce very similar results and both agree with the true class given by the convection score.

The right panel of Fig. 7 shows the same quantities as on the left panel but for 23 July 2013. ~~In contrast to the presented winter case , this case~~ This case indicates convective rain ~~represented at~~ falling between 15:00 UTC and 16:00 UTC. Z_{max} (h), $v_{\mathrm{D,max}}$ (i) and $\sigma v_{\mathrm{D,max}}$ (j) and the calculated convection score are characterized by high values representing convective rain. Figure 7 (l) ~~gives an impression on the attenuated equivalent reflectivity~~ shows the radar reflectivity factor of the shower~~and its short intense time span. Both methods~~. The PDF- and ANN method are in a very good agreement and classify each profile as convective in conformity with the convection score (truth).

The performance of both algorithms over a whole year (test data year 2014) is illustrated in Fig. 8. ~~The~~ It shows the relative frequency of occurrence of ~~the stratiform cases from~~ precipitation profiles that are defined by the convection score (truth) to be stratiform (a), inconclusive (b), or convective (c). For the PDF method cases are stated as stratiform when the f value is lower than -0.9, inconclusive when f is between -0.9 and 0.9, and convective when f is larger than 0.9. For the stratiform cases the PDF and ANN ~~values agrees well within a few percent . 23~~methods classify most stratiform cases to be stratiform (84.7 % and 96.1 % for ANN and PDF, respectively, see Fig. 8 ~~% of inconclusive cases classified by the ANN are contrasted by 13~~a). Only 15.3 % and 3.9 %, respectively, are erroneously classified as inconclusive. These are cases with higher convection scores with averaged values around roughly 2.5 which is closer to the transition of convection scores larger than 3 that are stated as inconclusive. As expected, neither ANN nor PDF misclassified true stratiform cases as convective. The performance of the classification of true convective cases (c) is very similar. There are almost no completely misclassified cases and only a few percent of erroneously inconclusive cases. Here the averaged convection scores are roughly 6 which means on the lower edge of the convective classification and close to the transition of convection scores of less than 5.5 that are stated as inconclusive. 85.8 % and 98.1 % (ANN and PDF) of the true convective cases are correctly classified as convective.

However, the most critical point is the classification of the true inconclusive cases (Fig. 8 ~~% from PDFmethod. The lower amount of inconclusive cases at the PDF method is~~ b). Only 71 % and 35.8 % (ANN and PDF) are correctly classified. That means that nearly 30 % of ANN-based profiles and nearly 65 % of PDF-based profiles of all true inconclusive cases are classified as stratiform or convective. The ANN is performing better here. This is caused by the ~~fact, that this class is actually not distinguished, since it is classified as uncertain stratiform convective discrimination (f value between -0.9 and 0.9~~strict convection score discrimination which was stated as truth. In fact, these inconclusive cases might be classified as stratiform or convective but the thresholds were chosen very strict to confidently separate two classes which are mainly free of misclassified rain events. The averaged convection score of the false stratiform inconclusive cases (ANN) amounts to 3.6 and of the false convective inconclusive amounts to 5 (Fig. 8 b). The ~~difference between both methods for convective cases amounts to 8 %.One has to consider~~ erroneously stratiform and convective classified inconclusive cases of the PDF method (25.9 % and 38.3 %) has averaged convection score values of 3.6 (stratiform) and 4.9 (convective). Apparently, these cases would be correctly classified in case of less strict convection score thresholds than currently used (3 and 5.5, see Fig. 2). It is expected to improve the ANN and PDF performances by gathering more data for algorithm training.

It has to be considered that the total amount of data is different for both methods. This is due to the fact that some combinations of the three input variables do not appear within the training data causing gaps in the ~~3D PDF~~3D-PDF. Those combinations cannot be classified ~~.~~but its amount is less than 0.2 % for the 2014 test data set.

5 Conclusions and outlook

In order to improve microphysical parametrizations within small-scale models one has to deal with large data sets. The presented rain type classification methods based on PDF and ANN algorithms are suited to process micro rain radar data from long time series and outperform traditional ~~convective~~ convection score methods. The effort of creating a robust training data set without unphysical data between both methods is similar and the application of both methods is straightforward. The main advantage of the ANN in contrast to the PDF method is that ~~inconclusive profiles can be classified~~ the ANN method was trained to directly classify inconclusive profiles which leads to a lower amount of false classified profiles.

In a next step, evaporative cooling rates will be estimated for convective rain events to parametrize the cooling by means of temperature, relative humidity and rain droplet number concentration. It is also planned to apply the algorithms to different ground-based remote-sensing sites that have long-term MRR observations to create stratiform-vs-convective rain event climatologies. At present, the new MRR of the University of Leipzig[5] is running 24/7. In the near future, the classification algorithms will be applied operationally and will be improved with continuously gathered data.

Code availability. The open source machine learning library for research and production TensorFlow (Abadi et al., 2015) used for this publication is available under https://www.tensorflow.org/, last accessed: 2020-12-01.

Author contributions. AF prepared the manuscript in close collaboration with HK. AF performed the investigations and data analyses. JZ and FL contributed with their knowledge about basic meteorology and convective indices. JZ also contributed with his experience in radar data analysis. The conceptualization was initialized by AF. All authors have contributed to the scientific discussions.

Competing interests. The authors declare that they have no conflict of interest.

[5]https://home.uni-leipzig.de/remsensarctic/index.php?lang=en&content=ql, last accessed: 2020-12-01

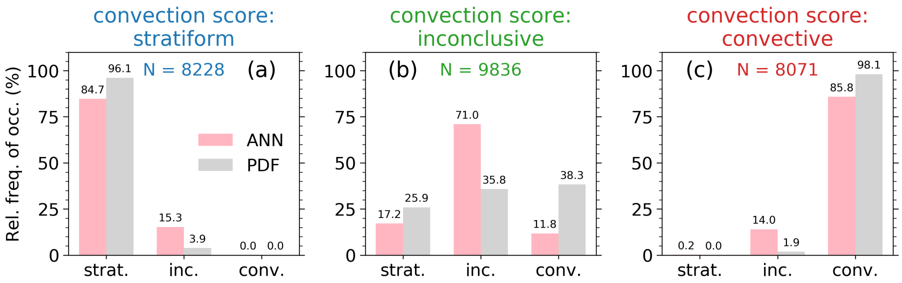

Figure 8. Relative ~~Frequency~~ frequency of occurrences of stratiform, inconclusive and convective rain classification for both ~~PDF~~ ANN (~~black~~light pink) and ~~ANN~~ PDF (grey) method separated by the true class (a,b,c) based on the test data 2014. The ~~color bar on the top indicates the confidence of the classification. The more blue or red the color~~ true class is defined by the ~~more confident the rain profile is classified as stratiform or convective~~strict convection score discrimination. The ~~dashed lines indicate the thresholds for stratiform and convective classifications. The~~ colored numbers denote the sample size. The numbers on top of each bar indicate the actual value.

Acknowledgements. This research has been supported by German Science Foundation (DFG) through funding the grants FO 1285/2-1, KA 4162/2-1 (PICNICC within the priority programme PROM) and WE 1900/33-1 and the Federal Ministry of Education and Research in Germany (BMBF) through High-Definition Clouds and Precipitation for advancing Climate Prediction research programme (HD(CP)2; FKZ: 01LK1504C and 01LK1502N). Data from JOYCE were provided by DFG-funded Core Facility (JOYCE-CF) under DFG research grant LO 901/7-1.

References

Abadi, M., Agarwal, A., Barham, P., Brevdo, E., Chen, Z., Citro, C., Corrado, G. S., Davis, A., Dean, J., Devin, M., Ghemawat, S., Goodfellow, I., Harp, A., Irving, G., Isard, M., Jia, Y., Jozefowicz, R., Kaiser, L., Kudlur, M., Levenberg, J., Mané, D., Monga, R., Moore, S., Murray, D., Olah, C., Schuster, M., Shlens, J., Steiner, B., Sutskever, I., Talwar, K., Tucker, P., Vanhoucke, V., Vasudevan, V., Viégas, F., Vinyals, O., Warden, P., Wattenberg, M., Wicke, M., Yu, Y., and Zheng, X.: TensorFlow: Large-Scale Machine Learning on Heterogeneous Systems, https://www.tensorflow.org/, software available from tensorflow.org, 2015.

Andersson, T., Andersson, M., Jacobsson, C., and Nilsson, S.: Thermodynamic indexes for forecasting thunderstorms in southern sweden, Meteorol. Mag., 118, 141–146, 1989.

Bacmeister, J. T., Suarez, M. J., and Robertson, F. R.: Rain Reevaporation, Boundary Layer–Convection Interactions, and Pacific Rainfall Patterns in an AGCM, Journal of the Atmospheric Sciences, 63, 3383–3403, https://doi.org/10.1175/JAS3791.1, https://doi.org/10.1175/JAS3791.1, 2006.

Caracciolo, C., Prodi, F., Battaglia, A., and Porcu', F.: Analysis of the moments and parameters of a gamma DSD to infer precipitation properties: A convective stratiform discrimination algorithm, Atmos. Res., 80, 165 – 186, https://doi.org/https://doi.org/10.1016/j.atmosres.2005.07.003, http://www.sciencedirect.com/science/article/pii/S0169809505002097, 2006.

Deng, M., Kollias, P., Feng, Z., Zhang, C., Long, C. N., Kalesse, H., Chandra, A., Kumar, V. V., and Protat, A.: Stratiform and Convective Precipitation Observed by Multiple Radars during the DYNAMO/AMIE Experiment, J. Appl. Meteorol. Clim., 53, 2503–2523, https://doi.org/10.1175/JAMC-D-13-0311.1, 2014.

Geerts, B. and Dawei, Y.: Classification and Characterization of Tropical Precipitation Based on High-Resolution Airborne Vertical Incidence Radar. Part I: Classification, J. Appl. Meteorol., 43, 1554–1566, https://doi.org/10.1175/JAM2158.1, 2004.

Ghada, W., Estrella, N., and Menzel, A.: Machine learning approach to classify rain type based on Thies disdrometers and cloud observations, Atmosphere, 10, 251, 2019.

Houze Jr, R. A.: Cloud dynamics, Academic press, Heidelberg, Germany, 2 edn., 2014.

Jergensen, G. E., McGovern, A., Lagerquist, R., and Smith, T.: Classifying Convective Storms Using Machine Learning, Weather Forecast., 35, 537–559, https://doi.org/10.1175/WAF-D-19-0170.1, 2020.

Kunz, M.: The skill of convective parameters and indices to predict isolated and severe thunderstorms, Nat. Hazard Earth Sys., 7, 327–342, https://doi.org/10.5194/nhess-7-327-2007, 2007.

Lazri, M. and Ameur, S.: Combination of support vector machine, artificial neural network and random forest for improving the classification of convective and stratiform rain using spectral features of SEVIRI data, Atmos. Res., 203, 118 – 129, https://doi.org/https://doi.org/10.1016/j.atmosres.2017.12.006, http://www.sciencedirect.com/science/article/pii/S0169809517309572, 2018.

Liu, Z., Vaughan, M. A., Winker, D. M., Hostetler, C. A., Poole, L. R., Hlavka, D., Hart, W., and McGill, M.: Use of probability distribution functions for discriminating between cloud and aerosol in lidar backscatter data, J. Geophys. Res. Atmos., 109, D15202, https://doi.org/10.1029/2004JD004732, 2004.

Liu, Z., Vaughan, M., Winker, D., Kittaka, C., Getzewich, B., Kuehn, R., Omar, A., Powell, K., Trepte, C., and Hostetler, C.: The CALIPSO Lidar Cloud and Aerosol Discrimination: Version 2 Algorithm and Initial Assessment of Performance, J. Atmos. Oceanic Technol., 26, 1198–1213, https://doi.org/10.1175/2009JTECHA1229.1, 2009.

Löhnert, U., Schween, J. H., Acquistapace, C., Ebell, K., Maahn, M., Barrera-Verdejo, M., Hirsikko, A., Bohn, B., Knaps, A., O'Connor, E., Simmer, C., Wahner, A., and Crewell, S.: JOYCE: Jülich Observatory for Cloud Evolution, Bulletin of the American Meteorological Society, 96, 1157–1174, https://doi.org/10.1175/BAMS-D-14-00105.1, 2015.

Maahn, M. and Kollias, P.: Improved Micro Rain Radar snow measurements using Doppler spectra post-processing, Atmos. Meas. Tech., 5, 2661–2673, https://doi.org/10.5194/amt-5-2661-2012, 2012.

Morrison, H., Tessendorf, S. A., Ikeda, K., and Thompson, G.: Sensitivity of a Simulated Midlatitude Squall Line to Parameterization of Raindrop Breakup, Monthly Weather Review, 140, 2437–2460, https://doi.org/10.1175/MWR-D-11-00283.1, https://doi.org/10.1175/MWR-D-11-00283.1, 2012.

Niu, S., Jia, X., Sang, J., Liu, X., Lu, C., and Liu, Y.: Distributions of Raindrop Sizes and Fall Velocities in a Semiarid Plateau Climate: Convective versus Stratiform Rains, J. Appl. Meteorol. and Clim., 49, 632–645, https://doi.org/10.1175/2009JAMC2208.1, 2010.

Pattnaik, S. and Krishnamurti, T. N.: Impact of cloud microphysical processes on hurricane intensity, part 2: Sensitivity experiments, Meteorology and Atmospheric Physics, 97, 127–147, https://doi.org/10.1007/s00703-006-0248-x, https://doi.org/10.1007/s00703-006-0248-x, 2007.

Peters, G., Fischer, B., and Anderson, T.: Rain observations with a vertically looking Micro Rain Radar (MRR) , Boreal Environ. Res., 7, 353–362, 2002.

Peters, G., Fischer, B., Münster, H., Clemens, M., and Wagner, A.: Profiles of Raindrop Size Distributions as Retrieved by Microrain Radars, 44, 1930–1949, https://doi.org/10.1175/JAM2316.1, 2005.

Rosenfeld, D., Amitai, E., and Wolff, D. B.: Improved Accuracy of Radar WPMM Estimated Rainfall upon Application of Objective Classification Criteria, J. Appl. Meteorol., 34, 212–223, https://doi.org/10.1175/1520-0450-34.1.212, https://doi.org/10.1175/1520-0450-34.1.212, 1995.

Rotstayn, L. D.: A physically based scheme for the treatment of stratiform clouds and precipitation in large-scale models. I: Description and evaluation of the microphysical processes, Quarterly Journal of the Royal Meteorological Society, 123, 1227–1282, https://doi.org/10.1002/qj.49712354106, 1997.

Schlemmer, L. and Hohenegger, C.: The Formation of Wider and Deeper Clouds as a Result of Cold-Pool Dynamics, Journal of the Atmospheric Sciences, 71, 2842–2858, https://doi.org/10.1175/JAS-D-13-0170.1, 2014.

Thompson, E. J., Rutledge, S. A., Dolan, B., and Thurai, M.: Drop Size Distributions and Radar Observations of Convective and Stratiform Rain over the Equatorial Indian and West Pacific Oceans, J. Atmos. Sci., 72, 4091–4125, https://doi.org/10.1175/JAS-D-14-0206.1, 2015.

Tokay, A. and Short, D. A.: Evidence from Tropical Raindrop Spectra of the Origin of Rain from Stratiform versus Convective Clouds, J. Appl. Meteorol., 35, 355–371, https://doi.org/10.1175/1520-0450(1996)035<0355:EFTRSO>2.0.CO;2, 1996.

Tokay, A., Short, D. A., Williams, C. R., Ecklund, W. L., and Gage, K. S.: Tropical Rainfall Associated with Convective and Stratiform Clouds: Intercomparison of Disdrometer and Profiler Measurements, J. Appl. Meteorol., 38, 302–320, https://doi.org/10.1175/1520-0450(1999)038<0302:TRAWCA>2.0.CO;2, https://doi.org/10.1175/1520-0450(1999)038<0302:TRAWCA>2.0.CO;2, 1999.

Williams, C. R., Ecklund, W. L., and Gage, K. S.: Classification of Precipitating Clouds in the Tropics Using 915-MHz Wind Profilers, J. Atmos. Ocean. Technol., 12, 996–1012, https://doi.org/10.1175/1520-0426(1995)012<0996:COPCIT>2.0.CO;2, https://doi.org/10.1175/1520-0426(1995)012<0996:COPCIT>2.0.CO;2, 1995.

Winker, D. M., Vaughan, M. A., Omar, A., Hu, Y., Powell, K. A., Liu, Z., Hunt, W. H., and Young, S. A.: Overview of the CALIPSO Mission and CALIOP Data Processing Algorithms, J. Atmos. Oceanic Technol., 26, 2310–2323, https://doi.org/10.1175/2009JTECHA1281.1, 2009.

Worden, J., Noone, D., Bowman, K., Beer, R., Eldering, A., Fisher, B., Gunson, M., Goldman, A., Herman, R., Kulawik, S. S., Lampel, M., Osterman, G., Rinsland, C., Rodgers, C., Sander, S., Shephard, M., Webster, C. R., Worden, H., science team, and data contributors, T. T. E. S.: Importance of rain evaporation and continental convection in the tropical water cycle, Nature, 445, 528–532, https://doi.org/10.1038/nature05508, 2007.

Yang, Y., Chen, X., and Qi, Y.: Classification of convective/stratiform echoes in radar reflectivity observations using a fuzzy logic algorithm, J. Geophys. Res. Atmos., 118, 1896–1905, https://doi.org/10.1002/jgrd.50214, https://agupubs.onlinelibrary.wiley.com/doi/abs/10.1002/jgrd.50214, 2013.

Yang, Z., Liu, P., and Yang, Y.: Convective/Stratiform Precipitation Classification Using Ground-Based Doppler Radar Data Based on the K-Nearest Neighbor Algorithm, Remote Sens., 11, 2277, https://doi.org/10.3390/rs11192277, 2019.